



Thermal neutron detection by means of Timepix3

A. Tamburrino^{1,2,3,a}, G. Claps^{2,3}, G. M. Contessa⁴, A. Pietropaolo^{2,3}, F. Cordella^{2,3}, V. De Leo^{2,3}, R. M. Montekali², M. A. Vincenti², V. Nigro², R. Gatto¹, D. Pacella^{2,3}

¹ Department of Astronautical, Electrical and Energy Engineering, Sapienza University of Rome, Piazzale Aldo Moro 5, 00185 Rome, Italy

² ENEA Frascati Research Center, via E. Fermi 45, 00044 Frascati, Italy

³ INFN Frascati National Laboratory (LNF), via E. Fermi 40, 00044 Frascati, Italy

⁴ Italian National Institute of Health, viale Regina Elena 299, 00161 Rome, Italy

Received: 28 June 2023 / Accepted: 11 October 2023

© The Author(s) 2023

Abstract Thermal neutron detection plays a crucial role in numerous scientific and technical applications such as nuclear reactor physics, particle accelerators, radiotherapy, materials analysis and space exploration. There are several challenges associated with the accurate identification and quantification of thermal neutrons. The present work proposes a detailed characterization of a Timepix3 (TPX3) detector equipped with a Lithium Fluoride (^6LiF) converter in order to study its response to thermal neutrons that are identified through the $^6\text{Li}(n,\alpha)^3\text{H}$ reaction. The TPX3-based test system has been installed at the HOTNES facility in ENEA and the analysis highlighted its excellent performance showing high effectiveness in the identification of neutrons through morphological analysis of tracks produced by alpha and triton particles, after accurate discrimination from the gamma background. With the use of Monte Carlo simulations, it has been demonstrated that the main contribution is due to tritons and its signal can be used effectively in the identification of thermal neutrons obtaining an efficiency of 0.9 % for 25 meV neutrons. This allows the TPX3 to have important applications as an environmental monitor for thermal neutrons. This monitoring system can be simply realized and is easy to manage because of its compact size and its digital acquisition that allows a real-time analysis.

1 Introduction

Thermal neutron detection represents a significant research and development area making it a valuable tool for ensuring greater safety and effectiveness in multiple scientific applications, including industrial and medical domains. Thermal neutron detection is achieved with different techniques depending on the particular application. These applications include neutron imaging, radiotherapy, nuclear fusion, neutron activation analysis (used in various fields such as geology, archaeology, material science, and space exploration), and so on. For many of these uses, it is important to provide a compact and real-time diagnostic system with good efficiency and optimal discrimination of the neutron signals against background. The present work introduces a compact detection system based on Timepix3 (TPX3) that can find useful applications in neutron radiation protection and neutron beam monitors. Timepix detectors have already been exploited in high-energy physics experiments to monitor thermal neutrons [1, 2]. The focus of the paper is the characterization of a TPX3 detector equipped with a layer of lithium fluoride (^6LiF), 95.5% enriched in the lithium-6 isotope, for thermal neutron detection. The measurements conducted at the HOTNES facility (ENEA Frascati) show a clear sensitivity of the device to 25 meV neutrons by identification of the reaction products (alphas and tritons). TPX3 has been developed by CERN-based Medipix collaboration [3] and falls into the family of complementary metal-oxide semiconductor imagers (C-MOS). This innovative technology is the basis of a new generation of detectors that exploits the possibility of direct detection of the charge released by particle interaction with the TPX3 material. It is different from other similar imaging devices that are based on indirect detection using scintillators or photoconductive cathode, such as the Charge Couple Devices (CCD) and systems based on Thin-Film-Transistors (TFT). In general, systems based on indirect conversion suffer degradation of the image due to the light spread from the scintillator and the presence of an unavoidable level of noise [4]. Instead TPX3 is a direct conversion system that requires lower power consumption with respect to other direct detection systems and the sensitive layer is separated and coupled to the read-out electronics by means of the bump-bonding technique (hybrid pixel readout). Each pixel can be read out individually by means of a dedicated read-out electronic channel that processes and digitalizes the signal, so the whole matrix can be managed with higher flexibility. Moreover, TPX3 are compact devices and, due also to the high spatial resolution, the interaction of a particle is registered as a track like for passive detectors (i.e. CR39), with a digital readout that provides the measurement of the released charge and position. The estimated measured efficiency of about 0.9% is reasonable when compared to detectors that have ^6LiF converters with

^a e-mail: antonella.tamburrino@uniroma1.it (corresponding author)

similar characteristics [5]. These properties make TPX3 suitable as a beam monitor for both neutron beams available at reactors (steady state) or accelerator-driven neutron sources (pulsed) for diagnostics purposes. As part of a research and development activity, one may foresee its possible use as an in-beam detection system for neutron imaging and radiography [6]. Additionally, it can serve as an environmental monitor for thermal neutrons, as an alternative to ^6Li -based scintillators. Although the latter have an efficiency on the order of 10%, the use of lower efficiency TPX3 is particularly useful in situations where beam intensity is significant, but available space to locate the detector is limited. This work also highlights that, unlike other similar neutron detectors, the TPX3 device allows online neutron discrimination with respect to background particles, and it is compact and inexpensive in comparison to CCD and scintillators.

2 Materials and methods

The experiment was performed with Cadmium Telluride (CdTe) Timepix3 equipped with 330 μm silicon deposited with a lithium fluoride (^6LiF) converter; the deposit was realized at ENEA Frascati. Before the experimental measurements, TPX3 has been characterized through an equalization procedure, a spatial uniformity study, and calibrated through a source of ^{241}Am . The used thermal neutron source is HOTNES (HOMogeneous Thermal NEutron Source) which will be presented in section 3.

2.1 Lithium fluoride converter

A polycrystalline lithium fluoride (LiF) film enriched to 95% with ^6LiF , nominal thickness 5 μm , was grown by thermal evaporation in controlled experimental conditions on a silicon substrate of dimensions $(14 \times 14) \text{ mm}^2$. The starting material consisted of commercially-available ^6LiF powder (Merck), heated at about 850 $^\circ\text{C}$ in a water-cooled tantalum crucible placed at the base of the steel vacuum chamber. The silicon substrate, cleaned with a procedure based on the use of detergents in ultrasonic baths, was fixed on a rotating substrate holder placed above the crucible at a distance of 22 cm. The pressure inside the vacuum chamber was below 1 mPa, prior to evaporation, while the substrate temperature was kept at 40 $^\circ\text{C}$ during the deposition process. The evaporation rate, fixed at 1 nm/s, and the film total thickness were monitored in situ by an INFICON crystal sensor.

2.2 CdTe Timepix3

TPX3 is the upgraded version of the previous TPX1 detector. Like its precursor, it is a hybrid pixelated detector (Fig. 1a) composed of an ASIC Timepix3 reading chip, based on C-MOS technology, bump-bonded on an active semiconductor sensor consisting of a 500 μm thick CdTe layer having an area of $14 \times 14 \text{ mm}^2$ and uniformly divided into a matrix of 256×256 pixels, each with an area of $55 \times 55 \mu\text{m}^2$ (Fig. 1b). The resulting assembly is mounted on a PCB board which manages the read-out functionality and provides the high voltage for the semiconductor bias.

Data acquisition has been carried out through the Katherine control module [7] and the software package called MMtrack [8]. In this case, TPX3 is an n-on-p type detector biased at -150 V in order to ensure an efficient charge collection and minimize the electronic noise. Ionizing particles reach the active volume passing through an Aluminum electrode layer (100 nm) that is used to polarize the detector producing an electron charge that drifts towards the pixel inducing a current pulse signal: each individual pixel is equipped with its own read-out electronics that is able to record the signal presence with a simultaneous measurement of transported charge and its time of arrival with respect to a software or hardware reference start time. Each pixel has a Charge

Fig. 1 a The CdTe TPX3 on its PCB board: the wire bondings can be observed, in particular those that provide the bias voltage; **b** layout scheme of a TPX3 section showing the active layer bump-bonded to the TPX3 chip where the induced signal is processed

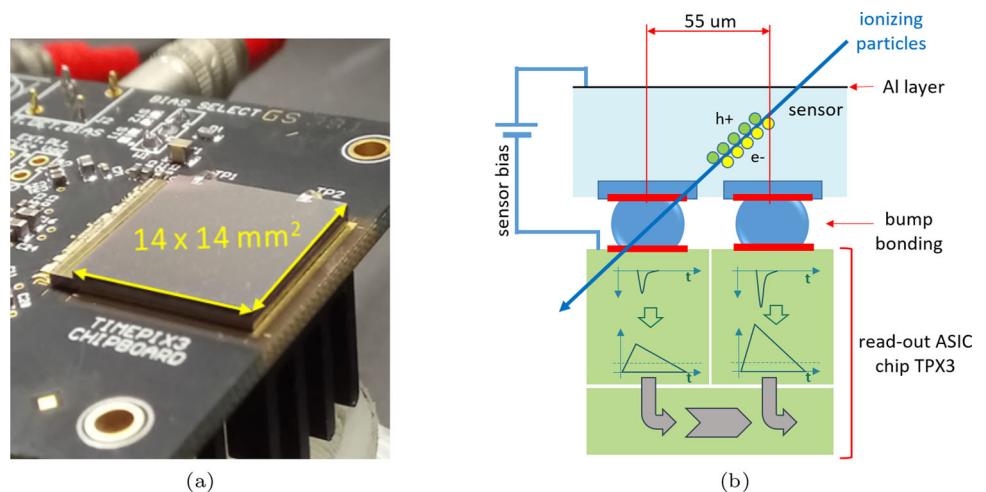
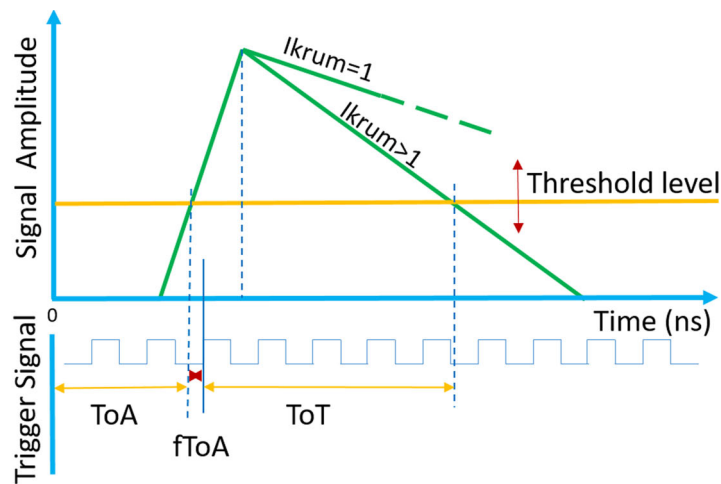
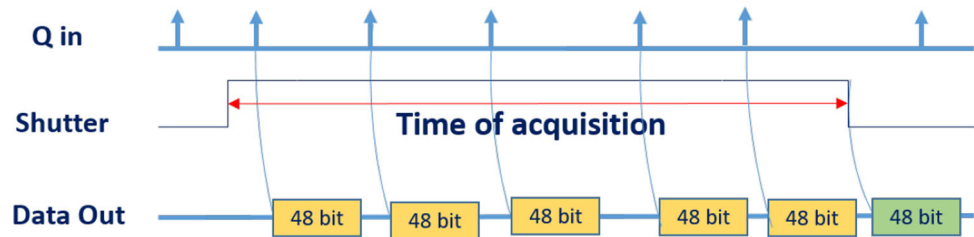


Fig. 2 **a** Layout schema of the TPX3 acquisition modes: the CSP provides an amplified triangular signal that is compared to a threshold level giving a measurement of ToA time (when the signal rises over threshold) and ToT counts (the time the signal is over threshold). The I_{krum} parameter manages the falling edge of the triangular signal; **b** layout schema of the data-driven acquisition mode: when the shutter is open, data coming from each pixel are transferred immediately and the pixels are again available



(a)



(b)

Sensitive Preamplifier (CSP) which acquires the current pulse caused by a particle interaction and creates a triangular output signal that is compared to a threshold level (Fig. 2a); the time elapsed above the threshold is measured as a digital count by a 40 MHz internal clock [9] and this is the ToT (Time over Threshold) mode that offers a digital measurement of the charge released. At the same time, when the rising edge of the CSP signal exceeds the threshold, the arrival time of the signal due to particle interaction is recorded and constitutes the Time of Arrival (ToA) of the particle with a maximum temporal resolution of 1.6 ns; ToA is compared to a software or hardware reference time.

The falling edge of the triangular signal is characterized by a time constant controlled by the I_{krum} (Krummenacher current) parameter: slower time constants correspond to low I_{krum} values and vice versa. As a consequence, the number of the ToT clocks can be tuned in order to not saturate the available digital scale. Timepix3 detector supports “data-driven” acquisition: in a set time window all switched-on pixels are transferred continuously so that all the particle flux can be followed in time. For each pixel, all data (pixel coordinates, ToT and ToA) are registered in a 48 bit word of which 10 bit are for ToT acquisitions (Fig. 2b). The ToA range can also cover longer time intervals until 10000 s from the acquisition start. A single pixel has a dead time of 450 ns and this value tends to increase with the number of activated pixels per unit time; however, in this work, the registered times are not affected by this dead time: the low flux measured does not give an additive contribution to the dead time and all data are registered correctly.

2.3 CdTe Timepix3 charge calibration

Before carrying out the calibration measurements the detector was subjected to a threshold equalization procedure and the minimum optimal threshold level was obtained by applying an additional value common to all the pixels to minimize the number of noisy pixels. Then some of the highly noisy affected pixels have been masked and not included in the acquisition. However, this procedure does not affect the data quality because of their negligible number in respect to all of the matrix pixels. A single particle interaction turns on a group of pixels (cluster) and, for each pixel, the ToT acquisition provides a measurement of a fraction of the released charge. Then the total charge released by a particle is measured by summing all the ToT contributions of the adjacent pixels; the result defines the ToT volume and is measured in clock counts (Fig. 3a). In this case, the response of the detector must be characterized for heavy particles and then an energy calibration procedure has been performed with alpha particles that produce clusters with tens of pixels. In order to remove the radiation background, clusters lower than two pixels have not been counted. In this case, an alpha

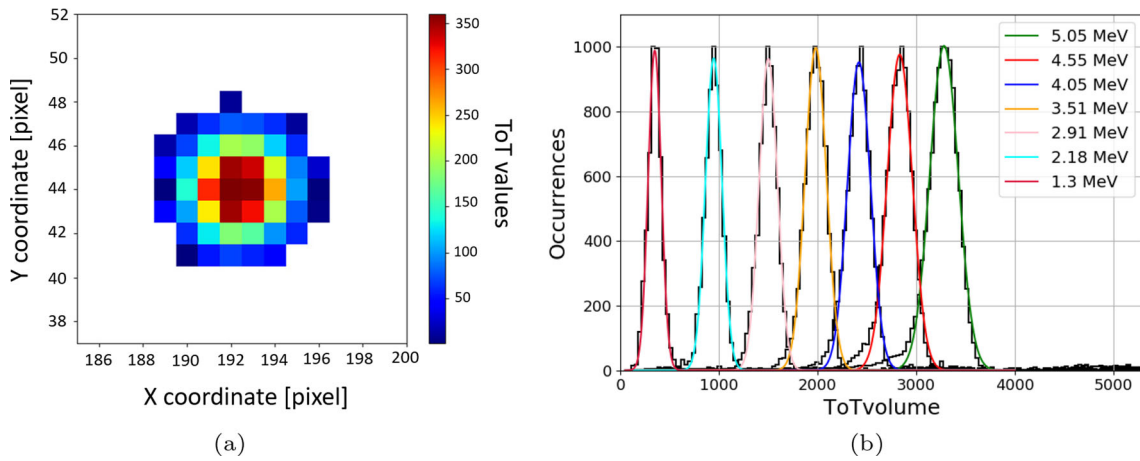
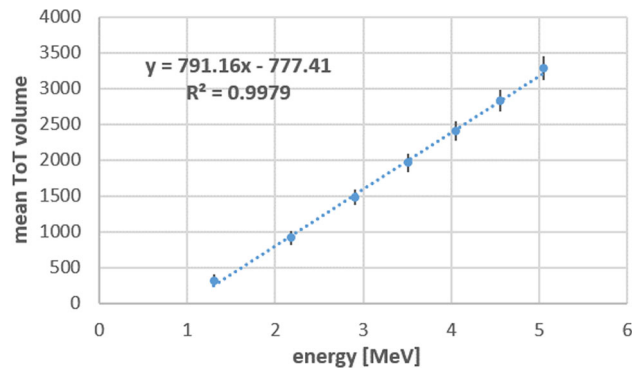


Fig. 3 **a** ToT values of a pixel cluster; **b** energy response at different distances of the alphas source (in black the normalized histograms of the experimental data and in other colors their gaussian fits)

Fig. 4 ToT energy calibration of TPX3 with high energy alpha particles from ²⁴¹Am



energy scan with ²⁴¹Am source was used in order to change alpha energies [10]; the source was placed on a linear stage by varying the distance from the detector surface with a step of 5 mm. Alpha particles are emitted by ²⁴¹Am with an energy of about 5.5 MeV; these particles lose energy interacting with air and energy spread increases as well, therefore with a scan of the source-to-detector distance we can produce different energies. Furthermore, a PVC mask with a 1 mm hole was used in order to select only the incident alphas in the perpendicular direction. In this way, seven energy values from 1.3 to 5.0 MeV have been obtained with a relative energy resolution between 9 and 5% for energies higher than 2 MeV (Fig. 3b).

The experimental setup was simulated with the CERN version of the Fluka Monte Carlo software [11] to estimate the alpha energy reaching the detector as a function of the source-to-detector distance (from 4.6 to 34.6 mm) and the simulated values have been correlated to the measured mean ToT values in order to obtain the energy calibration curve, as shown in the graph of Fig. 4:

As can be observed, for zero ToT the calibration curve for heavy particles reaches a minimum energy value of about 1 MeV that has been considered as the minimum cut-off energy to be applied also to the measurements on the reaction products coming from the neutron converter. Lower energies (in the keV range) are measured, but the calibration curve has a different slope [12].

3 Experimental measurements and data analysis

Experimental measurements have been performed on the HOTNES neutron source, a passive source based on Am-B. The neutron spectrum produced by the ²⁴¹Am-B source has its peak at about 3 MeV. The HOTNES source has been conceived to obtain a uniform neutron flux of thermal neutrons [13]. This has been realized by placing the Am-B source in the lower part of a cylindrical cavity with polyethylene walls. A layout scheme of the polyethylene structure (sketched in blue) containing the Am-B source is shown in Fig. 5a.

As can be observed, there is a polyethylene block in front of the source which has the role of thermalizing the energetic neutron together with the walls. As a result, a uniform neutron flux is produced inside the cylindrical cavity, in particular on some planes at defined distances from the source. The plane at 50 cm has been characterized and the measured neutron flux is approximately equal to 763 ± 11 neutrons/(cm² s), while the neutron spectrum has a peak at 25 meV, as shown in Fig. 5b.

Fig. 5 **a** General scheme of the HOTNES facility and TPX3 reference position on the iso-fluency surface at 50 cm from the source (red block); **b** neutron spectrum: open dots are the experimental values while the continuous line comes from MCNP simulation [14]

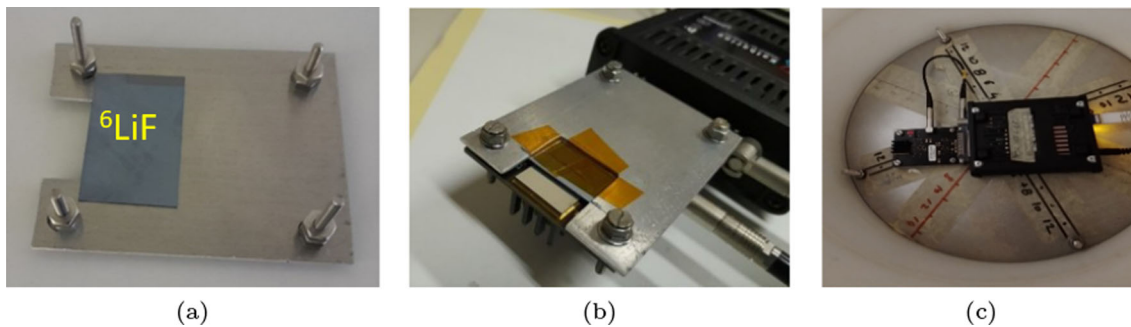
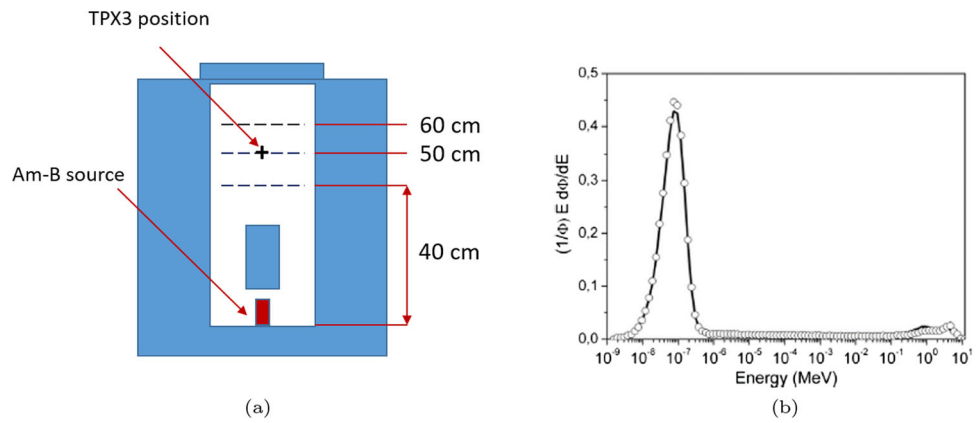
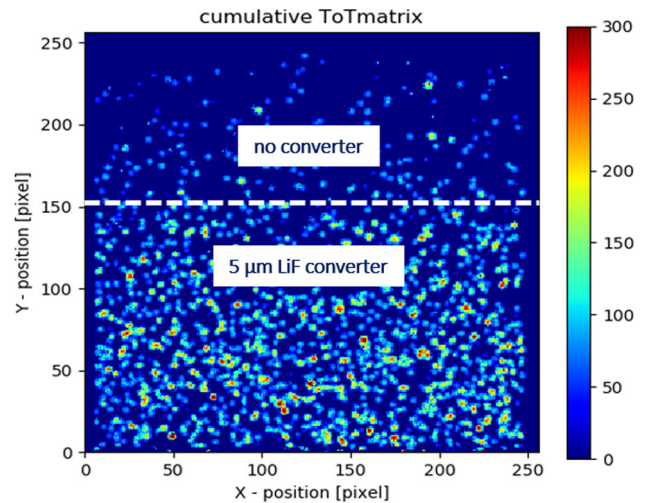


Fig. 6 **a** Aluminum mask with the silicon sheet deposited with the ^6LiF layer; **b** TPX3 equipped with aluminum mask: the upper area of TPX3 is not covered; **c** TPX3 with its control module Katherine after installation on aluminum support placed at 50 cm from the neutron source

Fig. 7 Image of the integrated response of the TPX3 device showing alpha and triton tracks registered in correspondence of the two different areas, with (below) and without (upper) converter. The number of observed tracks on the converter covered area is about one order of magnitude greater in respect to the not covered area



3.1 Measurements at the HOTNES facility and experimental results

For this experiment, the TPX3 has been equipped with an aluminum mask (Fig. 6a) that sustains the silicon substrate with the ^6LiF deposition side directed toward the TPX3 surface. Because of the presence of wire bonding, the silicon sheet is placed at a distance of 3 mm and, in order to study the effect of the converter, covers one-half of the TPX3 surface (Fig. 6b).

Then TPX3 with its Katherine control module has been placed on an aluminum plane support located 50 cm away from the Am-B source (Fig. 6c). The Katherine is controlled remotely through an Ethernet cable. For this type of measurement, the TPX3 has been biased at -150 V and 32 experimental runs were performed, each in data-driven mode with a time width of 900 s. The threshold has been set at the minimum value over the noise level and then there is no further cut on charge. The Ikrum value was set to a value of 15 because of the expected higher measured charges that can saturate the available digital scale. By selecting a temporal range of 300 s, the image of the integrated ToT is like the one shown in Fig. 7.

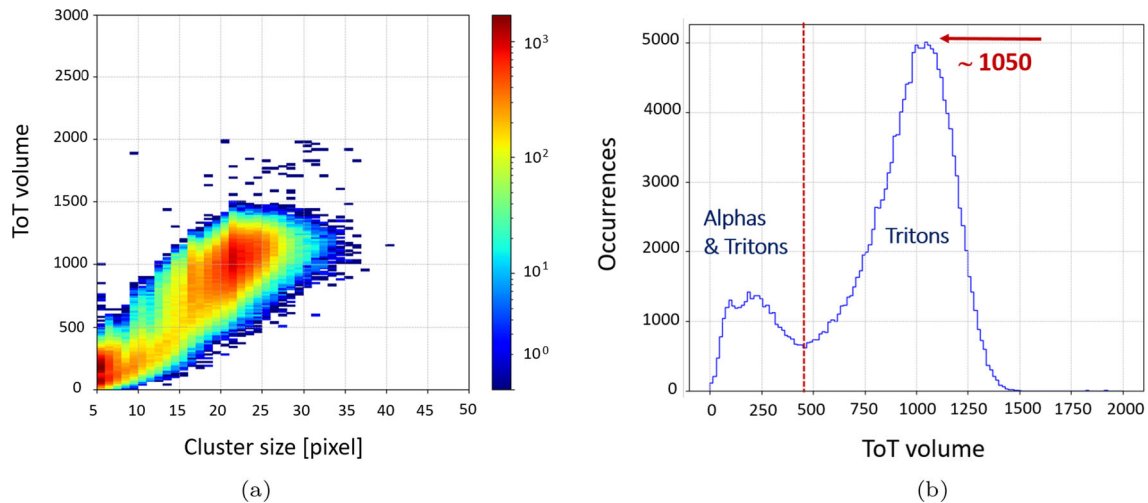


Fig. 8 **a** 2D plot distribution after application of thermal neutron filter cluster criteria for the measurement; **b** alpha and triton peaks in ToT volume distributions

It is clear that the number of cumulated tracks on the side with the converter is much more than those observed on the side without. In particular, tracks with a high number of pixels and high ToT volume are observed. In fact, depending on the type and energy of the interacting particle, the cluster assumes different shapes and, in order to allow the identification of the particles themselves, a series of morphological and charge parameters can be defined. In this case, three main parameters have been identified to discriminate the clusters due to reaction products: “cluster size” (CS), i.e. the number of adjacent pixels in a single cluster; the “ToT volume”, previously defined, and “Roundness” (Rnd), i.e. the ratio between the diameter of the circumference having the same cluster area and the length separating the two most distant pixels in the cluster. Using these parameters and by defining specific cuts on CS and Rnd it is possible to discriminate and identify the tracks of interest due to reaction products (alpha and triton particles) and remove the gamma and beta background. A series of tests on tracks morphology confirmed the same constraints on some parameters of previous works [15]: in this case, an optimal discrimination versus gamma and beta background is obtained with cuts on CS and Rnd respectively greater than 5 and 70. Using these cluster filter criteria the background was minimized and a good division between the signal below ${}^6\text{LiF}$ and the rest of the detector was achieved. Lower roundness values can be used, but there is a set of particles with CS below 10 that can be easily confused with gamma tracks. Therefore, the set roundness value was chosen in order to have a clear discrimination of alpha and triton tracks, even though this results in a decrease in efficiency. For this measurement, the ${}^6\text{LiF}$ region is well visible in figure 7. Applying these same constraints, in the ToT range between 1 and 2000, the 2D plot of ToT volume versus CS (Fig. 8a) shows three distinct populations and, in the histogram of ToT volume (Fig. 8b), a clear extended peak after a minimum is observed at high ToT values.

According to the calibration curve, the energy corresponding to this peak is approximately 2.3 MeV, while the energy of the minimum is about 1.5 MeV. Taking into account that alphas and tritons are produced over a 2π solid angle and undergo auto absorption inside the converter itself and in the air layer, it is expected that an energy of 2.3 MeV is consistent with the triton energy. Applying the same discrimination criterion (CS > 5 and Rnd > 70), the estimated measured efficiency is about 0.9%.

3.2 MC simulations and comparison with experimental data

The experimental set-up of the TPX3 board with the aluminum mask equipped with ${}^6\text{LiF}$ converter has been simulated using the MC Fluka code [11]. In this case a uniform neutron beam has been sent on the detector with an energy of 25 meV. Then the spectra of the alpha and triton particles entering the detector area were obtained in order to highlight the energetic contributions of the two reaction products (Fig. 9).

As can be observed, the simulated alpha spectrum is represented by a broad continuum that extends from 0 until 1.5 MeV, while the triton spectrum is localized to higher energies with a broad maximum from 2.3 to 2.5 MeV. These simulations are consistent with the experimental data and demonstrate that the main contribution to the experimental peak is due to triton interactions. Then the two observed main populations shown in Fig. 8 a are due to alphas and tritons together and only tritons, respectively. In the same plot, a mild population with higher CS and ToT volumes can also be observed, which has not been investigated but has a negligible weight for the efficiency measurements of the present work. According to these results, the simulated efficiency is 1.64%, equal to the sum of 0.47% from alphas and 1.17% from tritons. The calibration curve provides for a minimum measurable energy value on heavy particles of about 0.98 MeV, then applying this lower energy cut on the simulated spectra, the corrected simulated efficiency is 1.22%, the sum of 0.08% from alphas and 1.14% from tritons. Comparing the measured efficiency with the simulated one it finds that the presented simulation overestimates the measured efficiency by a factor of 1.3.

Fig. 9 Simulated alpha and triton spectra when the active area-converter distance is equal to 3 mm

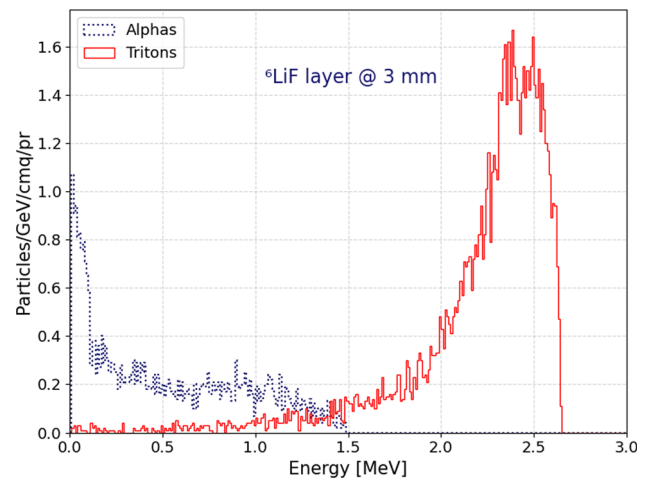
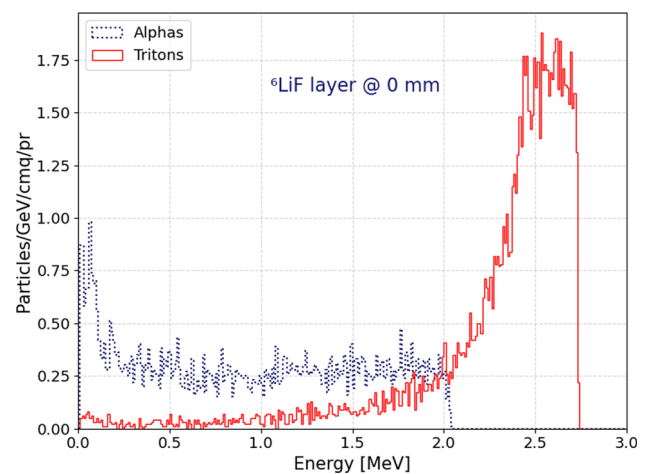


Fig. 10 Simulated alpha and triton spectra with ${}^6\text{LiF}$ deposited directly on TPX3 surface



4 Conclusion and future developments

TPX3 pixel detector coated with one layer of ${}^6\text{LiF}$ converter represents a good solution for thermal neutron investigation and can be successfully used for real-time measurements. In fact, this detector is a compact diagnostic system and presents relevant features: 2D configuration, simultaneous measurement of ToA and ToT with a high time resolution, high spatial resolution and count rate, clear sensitivity to thermal neutrons with rejection of background gamma particles and low-level noise (high ratio of threshold/noise). Moreover, CMOS technology with bump-bonding allows a direct measurement of the charge with the possibility to use different sensor materials (e.g. Si, GaAs, etc.). The use of ${}^6\text{LiF}$ converter layer is attractive thanks to the relatively high energy values of the reaction products; however, the effects of self-absorption limit the effectiveness of neutron detection and it is necessary to find solutions that allow an efficiency increase. According to the presented results, the neutron efficiency depends on converter mask properties, its positioning with respect to the chip, and the criteria applied to cluster analysis. An alternative way to improve efficiency is the deposition of the converter film directly on the surface of the TPX3; in this case, dedicated MC simulations (Fig. 10) demonstrate an increase in efficiency with a value of 1.7%, the sum of 0.4% from alphas and 1.3% from tritons.

At the moment, there are several ideas to improve efficiency by a converter in contact to TPX3 and an increase of converter's thickness as described in other works [16, 17]. The presented study demonstrates the possibility of realizing an effective monitor for thermal neutrons based on the innovative properties of TPX3. In the framework of radiation protection (for example, at nuclear or research sites) continuous monitoring of thermal neutrons is vital for safety and risk management and TPX3 could provide an effective and compact detection method. In addition, this type of device can be used for neutron diagnostics and imaging in materials science, art analysis and biomedical research. Compared to ${}^6\text{Li}$ -based scintillators, which can be bulky and require a large installation space, the TPX3, thanks to its small size, could be particularly useful in situations where the beam intensity is significant, but the available space is limited.

Funding Open access funding provided by Università degli Studi di Roma La Sapienza within the CRUI-CARE Agreement.

Data Availability Statements This manuscript has associated data in a data repository. [Authors' comment: Data will be made available on reasonable request to the authors.].

Open Access This article is licensed under a Creative Commons Attribution 4.0 International License, which permits use, sharing, adaptation, distribution and reproduction in any medium or format, as long as you give appropriate credit to the original author(s) and the source, provide a link to the Creative Commons licence, and indicate if changes were made. The images or other third party material in this article are included in the article's Creative Commons licence, unless indicated otherwise in a credit line to the material. If material is not included in the article's Creative Commons licence and your intended use is not permitted by statutory regulation or exceeds the permitted use, you will need to obtain permission directly from the copyright holder. To view a copy of this licence, visit <http://creativecommons.org/licenses/by/4.0/>.

References

1. B. Bergmann, T. Billoud, C. Leroy, S. Pospisil, Characterization of the radiation field in the atlas experiment with timepix detectors. *IEEE Trans. Nucl. Sci.* (2019). <https://doi.org/10.1109/TNS.2019.2918365>
2. P. Burian, P. Broulim, B. Bergmann, V. Georgiev, S. Pospíšil, L. Pušmana, J. Zicha, Timepix3 detector network at atlas experiment. *J. Instrum.* (2018). <https://doi.org/10.1088/1748-0221/13/11/C11024>
3. Medipix Collaboration (2004). <https://medipix.web.cern.ch/medipix/>
4. D. Pacella, Energy-resolved x-ray detectors: The future of diagnostic imaging. *Dove Press* **8**, 1–13 (2015). <https://doi.org/10.2147/RMI.S50045>
5. A. Pietropaolo, G. Verona Rinati, C. Verona, E.M. Schooneveld, M. Angelone, M. Pillon, A single-crystal diamond-based thermal neutron beam monitor for instruments at pulsed neutron sources. *Nucl. Instrum. Methods Phys. Res. A* **610**, 677–681 (2009) <https://doi.org/10.1016/j.nima.2009.09.013>
6. V. Merlo, M. Salvato, M. Cirillo, M. Lucci, I. Ottaviani, A. Scherillo, G. Celentano, A. Pietropaolo, Hybrid superconducting neutron detectors. *Appl. Phys. Lett.* (2015). <https://doi.org/10.1063/1.4915608>
7. P. Burian, P. Broulim, M. Jara, V. Georgiev, B. Bergmann, Katherine: Ethernet Embedded Readout Interface for timepix3. *J. Instrum.* (2017). <https://doi.org/10.1088/1748-0221/12/11/C11001>
8. IEAP Software Repository (2021). <https://software.itef.cvut.cz>
9. G. Claps, F. Murtas, L. Foggetta, C. Di Giulio, J. Alozy, G. Cavoto, Diamondpix: A CVD diamond detector with timepix3 chip interface. *IEEE Trans. Nucl. Sci.* **65**(10), 2743–2753 (2018). <https://doi.org/10.1109/TNS.2018.2871605>
10. J. Leidner, F. Murtas, M. Silari, Energy calibration of the Gempix in the energy range of 6 keV to 2 MeV. *J. Instrum.* (2021). <https://doi.org/10.1088/1748-0221/16/10/P10004>
11. FLUKA. <https://fluka.cern>
12. J. Jakubek, Precise energy calibration of pixel detector working in time-over-threshold mode. *Nucl. Instrum. Methods Phys. Res. A* (2010). <https://doi.org/10.1016/j.nima.2010.06.183>
13. A. Sperduti, M. Angelone, R. Bedogni, G. Claps, E. Diociaiuti, C. Domingo, R. Donghia, S. Giovannella, J.M. Gomez-Ros, L. Irazola-Rosales, S. Loreti, V. Monti, S. Miscetti, F. Murtas, G. Pagano, M. Pillon, R. Pilotti, A. Pola, M. Romero-Expósito, F. Sánchez-Doblado, O. Sans-Planell, A. Scherillo, E. Soldani, M. Treccani, A. Pietropaolo, Results of the first user program on the homogeneous thermal neutron source hotnes (enea/infn). *J. Instrum.* (2017). <https://doi.org/10.1088/1748-0221/12/12/P12029>
14. R. Bedogni, A. Sperduti, A. Pietropaolo, M. Pillon, A. Pola, J.M. Gómez-Rosa, Experimental characterization of hotnes: A new thermal neutron facility with large homogeneity area. *Nucl. Instrum. Methods Phys. Res. A* (2017). <https://doi.org/10.1016/j.nima.2016.10.056>
15. A. Tamburrino, G. Claps, F. Cordella, F. Murtas, D. Pacella, Timepix3 detector for measuring radon decay products. *J. Instrum.* (2022). <https://doi.org/10.1088/1748-0221/17/06/P06009>
16. A. Pietropaolo, F. Murtas, G. Claps, L. Quintieri, D. Raspino, G. Celentano, A. Vannozzi, O. Frasciello, A new ³He-free thermal neutrons detector concept based on the gem technology. *Nucl. Instrum. Methods Phys. Res. A* (2013). <https://doi.org/10.1016/j.nima.2013.06.058>
17. D.S. McGregor, M.D. Hammig, Y.-H. Yang, H.K. Gersch, R.T. Klann, Design considerations for thin film coated semiconductor thermal neutron detectors-i: basics regarding alpha particle emitting neutron reactive films. *Nucl. Instrum. Methods Phys. Res. A* (2003). [https://doi.org/10.1016/S0168-9002\(02\)02078-8](https://doi.org/10.1016/S0168-9002(02)02078-8)